The FluxEngine air-sea gas flux toolbox: simplified interface and extensions for *in situ* analyses and multiple sparingly soluble gases

Thomas Holding[1], Ian G. Ashton[1], Jamie D. Shutler[1], Peter E. Land[2], Philip D. Nightingale[2], Andrew P. Rees[2], Ian Brown[2], Jean-Francois Piolle[3], Annette Kock[4], Hermann W Bange[4], David K. Woolf[5], Lonneke Goddijn-Murphy[6], Ryan Pereira[7], Frederic Paul[3], Fanny Girard-Ardhuin[3], Bertrand Chapron[3], Gregor Rehder[8], Fabrice Ardhuin[3], Craig J. Donlon[9]

[1]University of Exeter, Penryn Campus, Cornwall, TR10 9EZ, UK.

[2]Plymouth Marine Laboratory, Prospect Place, Plymouth, PL1 3DH, UK.

[3]Ifremer, Univ. Brest, CNRS, IRD, Laboratoire d'Oceanographie Physique et Spatiale (LOPS), IUEM, Brest, France.

[4]GEOMAR Helmholtz Centre for Ocean Research Kiel, Marine Biogeochemistry Research Division, 24105 Kiel, Germany.

[5]International Centre for Island Technology, Heriot-Watt University, Stromness, Orkney, KW16 3AW, UK.

[6]Environmental Research Institute, University of the Highlands and Islands, Thurso, KW14 7EE, UK

[7]The Lyell Centre, Heriot-Watt University, Research Avenue South, Edinburgh, EH14 4AS, UK.

[8]Leibniz-Institute for Baltic Sea Research Warnemünde, 18119 Rostock, Germany.

[9]European Space Agency, Noordwijk, The Netherlands.

Correspondence to: Thomas Holding (t.m.holding@exeter.ac.uk)

Abstract. The flow (flux) of climate critical gases, such as carbon dioxide (CO_2), between the ocean and the atmosphere is a fundamental component of our climate and the biogeochemical development of the oceans. Therefore, the accurate calculation of these air-sea gas fluxes is critical if we are to monitor the health of the oceans and changes to the climate. FluxEngine is an open source software toolbox that allows users to easily perform calculations of air-sea gas fluxes from model, *in-situ* and Earth observation data. The original development and verification of the toolbox was described in a previous publication and the toolbox is already being used by scientists across multiple disciplines. The toolbox has now been considerably updated to allow its use as a Python library, to enable simplified installation, verification of its installation, to enable the handling of multiple sparingly soluble gases and greatly expanded functionality for supporting *in situ* dataset analyses. This new functionality for supporting *in situ* analyses includes user-defined grids, time periods and projections, the ability to re-analyse *in situ* CO_2 data to a common temperature dataset and the ability to easily calculate gas fluxes using *in situ* data from drifting buoys, fixed moorings and research cruises. Here we describe these new capabilities and then demonstrate their application through illustrative case studies. The first case study demonstrates the workflow for accurately calculating CO_2 fluxes using *in situ* data from four research cruises from the Surface Ocean CO_2 Atlas (SOCAT) database. The second case study calculates air-sea CO_2 fluxes using in situ data from a fixed monitoring station in the Baltic Sea. The third case study focuses on nitrous oxide (N_2O) and through a user defined gas transfer parameterisation identifies that

biological surfactants in the North Atlantic could suppress individual N_2O sea-air gas fluxes by up to 13%. The fourth and final case study illustrates how a dissipation-based gas transfer parameterisation can be implemented and used. The updated version of the toolbox (version 3) and all documentation is now freely available.

1. Introduction

The exchange of climate relevant gases between the oceans and atmosphere including that of carbon dioxide (CO_2), nitrous oxide (N_2O) and methane (CH_4) is a major component of the climate system, and the ability of the oceans to absorb and desorb these gases varies both temporally and spatially. The need to monitor this exchange has been the driver for international data collation initiatives such as the Surface Ocean CO_2 ATlas (SOCAT, (Bakker *et al.*, 2016)) and the MarinE MethanE and NiTrous Oxide database (MEMENTO, (Kock and Bange, 2015)). These collaborative efforts are now routinely collecting, quality controlling and collating over a million new *in situ* data points each year. FluxEngine complements these initiatives by providing a standardised tool, which can robustly calculate air-sea gas fluxes from such *in situ* data, with the flexibility to incorporate new data sources and methodologies. The use of common tools and methods simplifies collaborations and accelerates advancements, both within and between scientific disciplines, through eliminating methodological or implementation-driven differences and the duplication of effort.

1.0 Overview of FluxEngine

FluxEngine is a flexible open source toolbox that allows users to easily exploit Earth observation and model data, in combination with *in situ* data, to calculate air-sea gas fluxes (Shutler *et al.*, 2016). It is available to download from http://github.com/oceanflux-ghg/FluxEngine. The toolbox uses plain text-format configuration files allowing the user to configure the input data sources, the temporal period for the analysis, the structure of the air-sea gas flux calculation and user-defined gas transfer velocity parameterisations. Further optional features include the addition of random noise or bias to the input data. The calculation itself can be performed using fugacity, partial pressure or concentration data, via a user defined bulk formulation, including formulations that can account for vertical temperature gradients across the mass boundary layer, the very small layer at the surface over which gas exchange occurs. A full description of the differences between the different flux formulations is provided in (Shutler et al., 2016) and (Woolf et al., 2016). The formulation that enables vertical temperature and salinity gradients to be included allowing a more accurate gas flux calculation is described in detail by (Woolf et al., 2016) and takes the generalised form of

$$F = k(\alpha_W \, fG_W - \alpha_S \, fG_A) \tag{1}$$

where F is the sea-to-air flux of a sparingly soluble gas G, k is the gas transfer velocity, α_S and α_W are the solubilities of the gas above and below the surface water interface and fG_A and fG_W are the respective fugacities. Here we use 'p' and 'f' prefixes to refer to partial pressure and fugacity of a gas, respectively. Gas transfer velocity is driven by turbulence at ocean surface, caused by wind stress and wave breaking, amongst other processes. Because of the wide availability of high quality wind data products and the relative difficulty of directly measuring turbulence, it is commonplace to estimate k

using a statistical relationship with wind speed, e.g. (Ho *et al.*, 2006; Nightingale *et al.*, 2000; Wanninkhof, 2014).

Concentration of the gas is determined by its solubility and fugacity (or partial pressure). Equation (1) can therefore be rewritten as a product of the gas transfer velocity and the difference in gas concentrations,

$$F = k(G_W - G_S) \tag{2}$$

where G_S and G_W are the concentration of the gas above and below the interface. The FluxEngine configuration file allows users to choose the structure of the gas flux calculation, the inputs and the gas transfer velocity (either by choosing an already implemented published algorithm or through parameterising their own). The user can then perform calculations across their chosen input data and the outputs are Climate Forecast (CF) standard netCDF 4.0 files that contain data layers for each of the stages of the calculation, along with process indicator layers to aid the interpretation of the calculated gas fluxes (such as surface chlorophyll-a concentrations, the climatological position of temperature fronts and error indicator layers). A summary of the main features of the toolbox is given in Table 4 (appendix C).

Version 1.0 of FluxEngine was introduced and described by (Shutler *et al.*, 2016), which included a full description of the calculations, the flexibility of the toolbox, and the extensive verification of the different calculations along with examples of its use. Since its original release the toolbox has continued to be developed and extended based on feedback from the user communities and the needs of specific scientific studies (e.g. Ashton *et al.*, 2016). These developments have considerably extended the functionality of the toolbox and broadened the range of possible applications to which it can be applied. At the time of writing, the toolbox and resulting data have been used to quantify regional and global uncertainties (e.g. Wrobel and Piskozub, 2016; Wrobel, 2017; Woolf et al., 2019), evaluate the impact of gas transfer processes on regional and global gas exchange (e.g. Ashton *et al.*, 2016; Pereira *et al.*, 2018), evaluate the European shelf sea CO_2 gas-fluxes and sink (Shutler *et al.*, 2016) and investigate biological and physical controls of air-sea exchange (Henson *et al.*, 2018). FluxEngine has also been used to identify shortfalls of current modelling approaches through the inclusion of FluxEngine outputs within an international inter-comparison (Rödenbeck *et al*., 2015) and it is currently being used within two pan-European carbon monitoring research infrastructure projects (EU RINGO and EU BONUS INTEGRAL) which are part of the Integrated Carbon Observing System, ICOS. The toolbox has also been incorporated within undergraduate and postgraduate teaching (e.g. at the University of Exeter within geography, environmental science and marine biology degrees, and at Utrecht University for computer science). Most recently the toolbox is being used by two European Space Agency (ESA) projects to support preliminary studies for a new satellite concept (the Sea Surface Kinematics Multiscale Monitoring, SKIM, satellite mission (Ardhuin *et al.*, 2018)) and to verify the theoretical understanding of vertical temperature profiles and concentration gradients (as presented by Woolf *et al.*, 2016) through the analysis of a novel fiducial reference dataset. The results from these studies will be reported elsewhere, but their needs have driven some of the advancements presented here.

This paper uses four case studies to illustrate key developments and the extended capabilities now contained within version 3.0 of the FluxEngine toolbox. Collectively, the case studies illustrate user selectable grids, support for calculating sea-to-air gas fluxes from time series data collected by fixed monitoring stations and research cruises (and how to incorporate the flux outputs into the original dataset to create a coherent time series), and the ability to calculate nitrous oxide (N_2O) sea-to-air gas fluxes, the addition of a new forcing variable (kinetic energy dissipation rate). The extensive support for *in situ* data contained within version 3 of FluxEngine means that it can now be fully exploited by three different scientific communities in isolation: *in situ*, model and Earth observation; whilst the original capability to enable gas fluxes to be calculated from combinations of *in situ*, model and Earth observation data is retained.

Section 2 of this paper describes the structural extensions and changes, including the automatic software installers and verification tools (allowing users to verify the integrity of their installation). It also explains how the toolbox can now be used as a command line tool or as a Python library. Section 3 then presents the case studies, while section 4 outlines the future direction and developments for the toolbox and section 5 gives conclusions. To aid the user the Appendices of this paper provide a list all of the toolbox utilities (Sect. 6), details of all data sets used in the case studies (Sect. 7) and an overview of the main toolbox features and options (Sect. 8).

2. New capabilities

The following sections describe the extensions to the FluxEngine toolbox that are now contained within version 3.

2.1. Installation, verification and use

FluxEngine has now been optimised for use on a standalone desktop or laptop computer, removing the previous requirement for specialist computing facilities. Installation tools or instructions are provided for the following operating systems: Ubuntu/Debian based Linux (*install_dependendies_ubuntu.sh*), Apple Mac (*install_dependencies_macos.sh*) and Windows (instructions are within *FluxEngineV3_instructions.pdf*). Separate utilities (*verify_takahashi09.py* and *verify_socatv4_sst_salinity_gradients_N00.py*) can then be used to verify that FluxEngine has been successfully installed. These verification utilities run standard global sea-to-air CO_2 gas flux calculations and net integrated fluxes using the (Takahashi *et al.*, 2009) sea-to-air CO_2 flux climatology (for year 2000) and the Woolf *et al.,* (2019) Surface Ocean CO_2 Atlas (SOCAT, Bakker *et al.*, 2016) derived sea-to-air CO_2 flux reference dataset for year 2010. Both of these datasets are contained within Holding *et al*., (2018) and the verification process compares the output from a test run of the toolbox with the data in published reference data of Holding *et al.*, (2018). The installation is deemed successful if all results are identical to the reference dataset within a precision of 5 decimal places. An additional utility (*run_full_verification.py*) enables the user to perform a more detailed verification of different user defined options which exploits the Woolf *et al.*, (2019) reference dataset. This executes a suite of 12 different configurations and scenarios, the justification for which are described within Woolf *et al*., (2019). Owing to the large volume of data required to execute and verify all of these scenarios, the verification data are not packaged with the standard FluxEngine download, but are all freely available and contained within Holding *et al.*, (2018).

FluxEngine is now implemented as a Python module available on a creative commons license via http://github.com/oceanflux-ghg/FluxEngine. This means that FluxEngine and its accompanying utilities can be used as command line tools (stand-alone tools or called from another piece of software) or imported as a Python module and easily integrated with other software. This approach offers a larger degree of flexibility than offered by version 1 of the toolbox and supports advanced exploitation. For example, a simple Python script can be written to run a sensitivity analysis where ensembles of flux calculations are required without any need to modify the underlying FluxEngine software.

To provide an indication of the execution time a benchmarking analysis was performed using an Intel Core i5 2.7 GHz laptop processor with 8GB RAM running MacOS El Capitan. The automatic installation took ~3 minutes to complete and the basic verification script using the Woolf *et al*., (2019) reference dataset (involving a global one year analysis of the gas fluxes for 2010, monthly temporal resolution and $1° \times 1°$ spatial resolution) took approximately 6 minutes to complete. As the flux calculation is sequential for each grid cell the execution time scales approximately linearly with number of grid points and number of time steps. Hence, doubling the temporal resolution will approximately double the execution time, whilst doubling the resolution of both spatial dimensions will lead to a factor of four increase in execution time.

2.2. Flexible input data specification

Previous versions of FluxEngine required the user to make changes to the underlying software in order to use new or differently formatted sources of input data. This required additional (and time consuming) testing and verification after modifications were made, making FluxEngine less accessible to those unfamiliar to Python programming. Two features have been added in version 3.0 to address this issue: i) file pattern matching (through standard Unix glob patterns and custom date/time tokens, described fully in *FluxEngineV3_instructions.pdf*) allows input file name format and directory structure to be customised using the plain text configuration file, ii) optional pre-processing functions can be used to manipulate input data after the data have been read into memory. These features can be specified for each input variable in the configuration file and FluxEngine contains a selection of common pre-processing functions, such as unit conversions or matrix transformation of the input data. Additional custom pre-processing functions can be added and tested easily by the user without the need to modify the core FluxEngine software, through copying and then completing the Python template function provided within the source code (*data_preprocessing.py*). Storing the completed function into the *data_preprocessing.py* file will then result in the custom pre-processing function being automatically available for use in any configuration files.

These features make it possible to use any observational netCDF dataset by specifying the file path and, if required, appropriate pre-processing functions. For example a custom pre-processing function could resample the input files, followed by a transformation to change the projection. This flexibility is conceptualised by the diagram in Fig. 1.
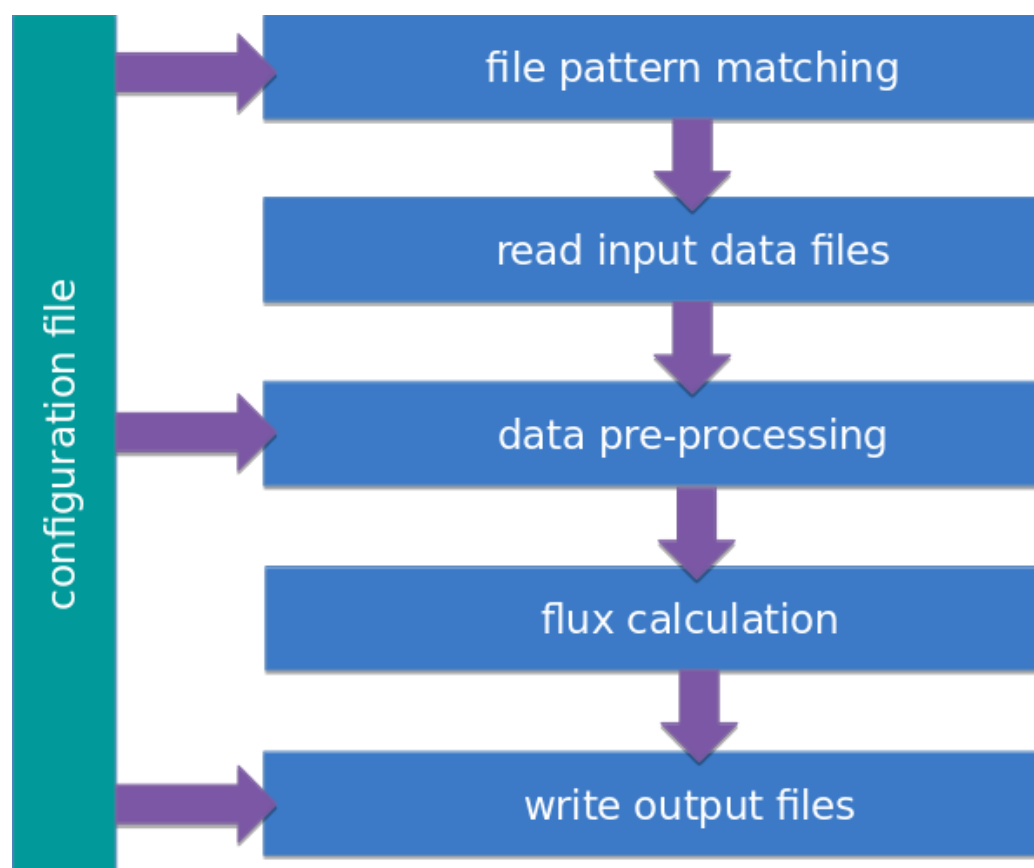
Figure 1: Conceptual diagram showing the way that input data are imported and used by FluxEngine. Single or groups of files are specified using a plain text configuration file. File names are interpreted using a subset of regular expression matching syntax (Unix glob patterns) and additional tokens are used to substitute time and date. The data pre-processing steps occur after input files are read into memory. Pre-processing functions are specified in the configuration file. Finally, the netCDF output files follow a user-specified filename and directory structure (as specified in the configuration file).

215

2.3. Extensive support for *in situ* data analyses

Version 1 of FluxEngine required that all input data be supplied as monthly $1° \times 1°$ global grids. These constraints restricted its relevance to regional analyses and *in situ* analyses, where sub-daily or sub-km resolutions are often more appropriate. The spatial resolution and extent can now be fully specified by
220   the user and regional masks can be used in conjunction with the *ofluxghg_flux_budgets.py* tool to calculate regional net integrated fluxes. In addition, flexible start and stop times and user-specified temporal resolution allows gas fluxes to be calculated for specific time intervals, e.g. the calculation can be configured to match the temporal resolution of the *in situ* data. Furthermore, a new configuration option allows output from multiple time points to be grouped into a single netCDF file
225   (rather than multiple files, one for each time point). This feature is designed to enable the calculation of gas fluxes from fixed research stations and other scenarios in which it is more convenient to provide results as a single time-series.

Improvements have been made to the bundled file conversion utilities, which convert between plain
230   text data formats and the netCDF format used by FluxEngine. By default, these tools use the SOCAT format (Bakker *et al.*, 2016) for convenience, but now offer a high degree of flexibility to reflect the variety of data formats and conventions used for storing *in situ* data. This means that the tools can be

used with virtually any text formatted *in situ* data files, avoiding the need for the user to convert their data to a fixed format with predefined column names.

235

The new utility, *append2insitu.py*, is designed specifically for use with *in situ* data and appends FluxEngine output as new columns within the original *in situ* data (achieved by matching spatial and temporal coordinates). For example, this means that users can use SOCAT (or custom) formatted *in situ* data as input to FluxEngine and then the results can be placed into a copy of the original input file,

240 allowing the user to study the calculated fluxes, gas transfer rates, gas concentrations etc. alongside (and aligned with) their original *in situ* data. This functionality is demonstrated in case studies one and three within this paper.

2.4. Reanalysis of *in situ* CO_2 fugacity data to a consistent temperature and depth

245 A new utility, *reanalyse_socat_driver.py*, is CO_2 specific and exploits a reference SST dataset (e.g. climate quality Earth observation SST data) and the original paired *in situ* measurements of CO_2 fugacity, fCO_2 and temperature to re-calculate the fCO_2 for the reference temperature dataset (and thus a consistent depth). The reasoning for the reanalysis is to reduce uncertainty and unknown biases that arise due to the fCO_2 measurements being collected using different instrumentation at some unknown

250 and potentially variable depth below the surface. A detailed justification of the method and a full description of the approach are described in Goddijn-Murphy *et al.*, (2015).

The reanalysis step is especially important if *in situ* data consisting of a collated dataset (originating from different instruments, sampling strategies or sources) is being used to calculate temporally

255 averaged gas fluxes (e.g. monthly mean values). In this situation the *in situ* measurements are highly likely to be collected from a range of different depths and unlikely to fully capture the monthly mean conditions of temperature and fCO_2 (due to aliasing). Whereas temporally averaged (mean) satellite observations are likely to provide a better representation (reference) of the mean temperature conditions. Therefore re-analysing the collated fCO_2 dataset to this reference temperature enables the

260 calculation of the equivalent mean fCO_2 data.

It is worth noting that ship draught, and thus underway measurement intake depth, can even vary on a single research cruise due to changes in sea state, ballasting or cargo. So the method can also be important for data collected during a single research cruise.

265

For the case studies presented here the satellite observed SST data used for the reanalysis are valid for a depth of ~1 m (Reynolds et al. 2007). So the re-calculated fCO_2 are therefore also valid for this depth, and are used to represent the conditions at the bottom of the mass boundary layer or sub-skin

temperature. The reanalysis to a consistent depth also enables a more accurate calculation of the gas

270   fluxes, as it is then possible to accurately calculate two solubilities and thus two concentrations, one at

the bottom, and one at the top of the mass boundary layer.

The Goodijn-Murphy et al., (2016) re-analysis method relies upon variations in fCO_2 being purely

isochemical. This assumes that the total dissolved inorganic carbon is approximately constant

275   throughout the surface waters over the temporal period and spatial scale being studied, and that

differences in fCO_2 are solely due to temperature differences altering the equilibria of the carbonate

system. Therefore caution should be used when applying the reanalysis method to data where these

assumptions are not valid.

280   The slow re-equilibrium time of CO_2 in seawater (i.e. on the order of months for CO_2 to equilibrate

with the atmosphere) ensure that monthly mean, or rolling monthly mean (centred on the day of

interest) skin or sub-skin sea surface temperature (SST) values are suitable for re-analysing the *in situ*

data. Arguably for re-analysing individual *in situ* datasets (e.g. to calculate gas fluxes for a single cruise

dataset) a robust daily skin or sub-skin SST value would be better, even if that is obtained by a seasonal

285   curve fitted to the monthly values and interpolated to the day of interest. Another solution would be to

collect paired measurements of skin SST, and fCO_2 and SST at depth, all *in situ*, as has been done on a

recent research cruise (Tarran, 2018) as ship-ready instruments are available, e.g. the Infrared Sea

surface Autonomous Radiometer (ISAR, Donlon *et al.*, 2008). This enables the paired measurements at

depth to be re-analysed using the *in situ* skin SST. However in the majority of cases ships collecting

290   fCO_2 data do not collect skin data. Where *in situ* skin temperature data are not available and satellite

temperature data are not appropriate, a regional model could be used to estimate skin temperature from

the SST a few metres below the surface. An example model capable of this is the US National Oceanic

and Atmospheric Administration (NOAA) Coupled Ocean-Atmosphere Response Experiment

(COARE) model (e.g. see Fairall *et al.*, 1996).

295

Whilst the reanalysis method and utility is CO_2 specific, its applicability to alternative gases (including

unreactive N_2O and CH_4) is discussed and shown in Table 1 of (Woolf *et al*., 2016). The impact on the

net gas fluxes of not performing this reanalysis on a relatively large time series of CO_2 measurements

through the north and south Atlantic is demonstrated within case study one (Sect. 3.1), whereas the

300   impact on global net integrated gas fluxes has been analysed by Woolf *et al.*, (2019).

A typical workflow for calculating sea-to-air gas fluxes from *in situ* data using FluxEngine, and the tools used at each step, is illustrated in Fig. 2. All of the *in situ* analysis utilities, including the use of the *reanalyse_socat_driver.py* tool, are demonstrated in case studies one to three (Sect. 3).

305
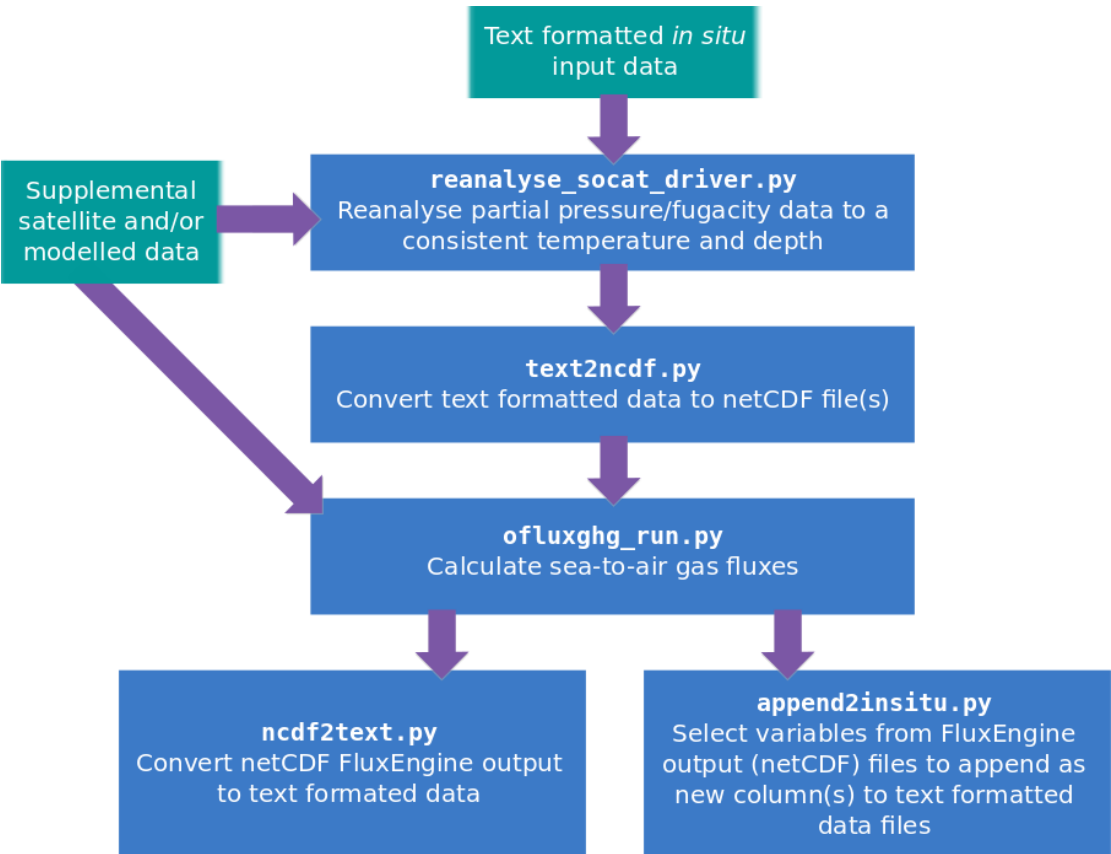
Figure 2: A typical CO₂ workflow for using FluxEngine with *in situ* data, showing the different utilities (blue boxes) and input data (green boxes) used at each stage.

2.5. Custom gas transfer velocity parameterisation

The processes that govern exchange, their relative importance and how gas exchange should be

310 parameterised are all active areas of research. e.g. Pereira *et al.*, (2018); Wrobel and Piskozub, (2016).

FluxEngine has always allowed users to select or define different gas transfer velocity parameterisations. However, version 3.0 adopts a modular approach to specifying the flux calculation, which makes it simpler for the user to extend the functionality and incorporate new gas transfer

315 parameterisations. Custom parameterisations can be implemented as separate Python classes without modifying the core FluxEngine software. This is achieved by copying and modifying the template class provided in *rate_parameterisation.py*. Storing the new class within *rate_parameterisation.py* means that the new parameterisation will be automatically available for inclusion in the configuration file. These custom parameterisations can define new input variables and therefore make use of additional

320 input data sources. These custom parameterisations can also produce new data layers in the final netCDF output, such as the results from intermediate calculation steps, which may be useful for testing or subsequent analysis outside of FluxEngine. Examples of how to use this functionality are provided in the source code. The toolbox documentation describes the process of, and best practices for, extending FluxEngine in this way (see Sect. 9.1 and 9.2 within *FluxEngineV3_instructions.pdf*).

325

This increased flexibility means that users can define and use region-specific gas transfer parameterisations or incorporate new transfer processes into existing gas transfer parameterisations (such as the impact of biological surfactants as discussed by Pereira *et al.*, 2018). Case studies one (Sect. 3.1) and two (Sect. 3.2) demonstrate the use of different well known wind speed based gas

330 transfer parameterisations, while case study three (Sect. 3.3) demonstrates the use of a custom gas transfer velocity parameterisation, which is used to assess the impact of biological surfactants on the N_2O gas fluxes. Case study four (Sect 3.4) utilises a gas transfer velocity parameterisation that is based on turbulent kinetic energy dissipation and provides an example of using additional input data.

335 **2.6. Extensions for other sparingly soluble gases**

The toolbox now supports the handling of two other sparingly soluble gases, (CH_4 and N_2O), and so gas specific data can be substituted into Eq. (1) or Eq. (2) (dependent upon the choice of setup). FluxEngine can calculate dissolved gas concentration from these gas input data, which can be supplied as either partial pressure or mean molar fraction of a gas in the dry atmosphere. Alternatively, dissolved

340 gas concentrations can be provided directly as an input. Gas specific parameterisations for Schmidt number (Sc) and solubility (α) are automatically chosen from those provided in Wanninkhof, (2014). The option to use the older Sc and α parameterisations from Wanninkhof, (1992) is also included for compatibility with previous versions and to aid comparative analysis. It is worth noting that both sets of Sc parameterisations are only valid for saline water, and care should be taken when using them for

345 analysis of freshwater data, or regions with low salinity (e.g. the Baltic Sea, see case study two, Sect. 3.2). Support for additional and user-defined Schmidt number parameterisations are likely to be added in the future.

350 **3. Case study examples of the new capabilities**

The following sections describe the application and results from four case studies that illustrate the new capabilities. Table 1 summarises the new features that are demonstrated in each case study. These case studies were run using FluxEngine version 3.0 which can be accessed via the GutHub repository's releases page: http://github.com/oceanflux-ghg/FluxEngine/releases/. It is advisable to always use the

355 most up-to-date version of FluxEngine which can be found via http://github.com/oceanflux-ghg/FluxEngine. The configuration files for each case study are included as examples in the *configs* sub-directory of the GitHub repository and these will be updated to maintain compatibility as new versions of the toolbox are released. In addition, interactive iPython Jupyter notebook tutorials for the first three case studies are included in the *tutorials* sub-directory of the repository. Section 4 of this

360 paper provides more information about these tutorials.

	New features utilised
Case study 1: Calculating sea to air CO_2 gas fluxes from ship research cruise data and using SOCAT data.	Flexible input data specification to select *in situ* data files and unit conversion using pre-processing functions (Sect. 2.2).
	Utilises new support for *in situ* data analysis,

	including the use of the *text2ncdf.py* and *append2insitu.py* tools, custom temporal resolution, reanalysis of fCO_2 to a consistent temperature field.
Case study 2: Calculating sea to air CO_2 gas fluxes from the Östergarnsholm fixed monitoring station data.	Flexible input data specification to select *in situ* data files and unit conversion using pre-processing functions (Sect. 2.2). Utilises new support for *in situ* data analysis, including use of *text2ncdf.py*, daily temporal resolution and output formatted as time-series (Sect. 2.3).
Case study 3: Surfactant suppression of sea to air N_2O gas fluxes using the MEMENTO data.	Flexible input data specification and unit conversion using pre-processing functions (Sect 2.2). Utilises new support for *in situ* data analysis, including use of the *text2netcdf.py* and *append2insit.py* tools, custom temporal resolution and cruise-specific time interval (Sect. 2.3). Custom gas transfer parameterisation (Sect. 2.5). Calculation of N_2O gas fluxes (Sect. 2.6).
Case study 4: Gas transfer velocity parameterisation using turbulent kinetic energy dissipation rate.	Unit conversion and use of custom pre-processing functions to calculate the dissipation rate from the input data. This uses the pre-processing functions to perform a non-trivial computation (Sect. 2.2). Use of a custom gas transfer parameterisation which includes the specification of an additional input data layer (Sect. 2.5).

Table 1: Summary of the new functionality demonstrated in each case study.

3.1 Case study 1: Calculating CO_2 fluxes from research cruise data

Each year over 1 million new *in situ* data points are included within the annual updates to the SOCAT dataset. Field scientists collecting these data often need to calculate the coincident sea-to-air gas fluxes, either using solely *in situ* measurements or through combining them with satellite Earth observation and/or model data.

370   Here we illustrate the procedure for calculating sea-to-air gas fluxes from *in situ* data collected during four different sampling campaigns. These *in situ* data (Kitidis and Brown, 2017; Schuster, 2016; Steinhoff *et al.*, 2016; Wanninkhof *et al.*, 2016) were all collected in the north Atlantic during October 2013. These are hereafter referred to as cruises 1-4, respectively. The *in situ* data were first downloaded from PANGAEA (an open access data publishing and archiving repository, http://www.pangaea.de) in

375 tab-delimited format. The datasets follow the standard SOCAT structure and content (see Bakker *et al.*, 2016 table 9).

The majority of the measurements needed for the sea-to-air CO_2 gas flux calculation were included within the downloaded datasets. The aqueous fCO_2, salinity, SST and air pressure were measured *in*

380 *situ* and the molar fraction of CO_2 in dry air (xCO_2) had been extracted from the GLOBALVIEW-CO_2 dataset (GLOBALVIEW-CO2, 2013). However, wind speed (needed for calculating the gas transfer velocity) was missing in all cases. Therefore, to complement these *in situ* data, multi-sensor merged wind speed data at 10 m were downloaded (Cross-Calibrated Multi-Platform, CCMPv2, 6 hour temporal resolution, $0.25^{\circ} \times 0.25^{\circ}$ spatial grid (Atlas, *et al.*, 2011)). These wind speed data were

385 appended to the *in situ* data by matching each *in situ* measurement to the closest temporal and spatial grid point. This same process was used to add columns for the second and third moments of wind speed, which were estimated by taking the second and third power of wind speed, respectively.

Two datasets (Schuster, 2016; Steinhoff, *et al.*, 2016) were missing xCO_2 data, and so the same method

390 of matching temporal and spatial grid points was used to fill in these fields using the GLOBALVIEW CO_2 dataset from the US National Oceanic and Atmospheric Administration (NOAA) Earth System Research Laboratory (ESRL) (GLOBALVIEW-CO2, 2013). For ease, these additional wind speed and xCO_2 data were downloaded, extracted and then inserted into the tab delimited *in situ* file using some simple custom Python scripts but the same process could be performed manually. These scripts are not

395 part of FluxEngine.

Collectively the *in situ* data from these cruises were collected from different ships and underway systems, all sampling water at different and unknown depths. These measurements are typically collected from a few metres below the water surface, whereas the CO_2 concentration (combination of

400 fCO_2 and solubility) on either side of the mass boundary layer is required for an accurate gas flux calculation. Before these data from multiple sources can be used for an accurate gas flux calculation, they need to be reanalysed to a common temperature dataset and depth (Goddijn-Murphy et al., 2015; Woolf et al., 2016). Therefore, the *reanalyse_socat_driver.py* tool was first used to reanalyse all fCO_2 data to a consistent temperature and depth.

405

Monthly mean sea surface temperatures from the Reynolds Optimally Interpolated Sea Surface Temperature dataset (OISST, Reynolds *et al.*, 2007) were used as the reference sub-skin temperature dataset, resulting in reanalysed fCO_2 that are valid for ~1 m and used to represent the bottom of the mass boundary layer (termed sub-skin within Woolf *et al.*, 2016).

410

The reanalysed fCO_2 were then inserted into the tab-delimited *in situ* dataset producing a single dataset. The tab-delimited file was then converted into a netCDF format file using the *text2ncdf.py* tool. This tool groups all data according to a user-specified spatial sampling grid, calculating the mean value and

standard deviation for each cell within the grid as well as the number of data that were used to calculate

415 these statistics. The spatial resolution was defined as $1° × 1°$ grid and FluxEngine was then configured to use each of the variables in the resulting netCDF file as input, with a pre-processing function applied to convert Reynolds OISST from Celsius to Kelvin (as all SST data within the main flux calculation use Kelvin). In order to produce a single netCDF output file for the entire 35 day period the temporal resolution for the flux calculation was set to 35 days. This allows the cruise tracks from all four cruises

420 (1-4) to be easily visualised at the same time.

The sea-to-air CO_2 fluxes were then calculated using the rapid model (see Eq. (1) and Woolf *et al.*, 2016) and was run using a quadratic wind speed based gas transfer velocity parameterisation (Ho *et al.*, 2007). To identify the impact of the fCO_2 reanalysis stage, the sea-to-air CO_2 flux calculation was

425 repeated using the original *in situ* SST and fCO_2.

Figure 3a shows the resultant calculated CO_2 flux along each of the cruises (1-4). The southern sub-tropical part of the cruise track 1 represents an area of the ocean that is a sink of CO_2 (negative sea-to-air flux). The northern sub-tropical section of cruise 1 shows an overall positive CO_2 flux into the

430 atmosphere, while south of 15°N the net fluxes are smaller and in variable direction. Interestingly, there are also examples (e.g. along the equatorial part of cruise track 1 and the western part of cruise track 2) where the direction of the flux has changed as a result of re-analysing the fCO_2 data. The highest magnitude fluxes were seen around the European continental shelf in cruise track 3, with a strong ocean sink west of Ireland and an intermittent source of CO_2 in the North Sea. Figure 3b shows the

435 difference in calculated net flux between use of the original fCO_2 data and the reanalysed fCO_2. Whilst very little difference is seen over large lengths of cruise tracks 1, 2 and 4, there are substantial differences in net flux of up to 0.1 C m^{-2} day^{-1} in some regions, for example within the frontal regions at the edge of the European shelf seas (cruise track 3) or in the southern section of cruise track 1. These are regions where temporally and spatially dynamic temperature gradients can exist that are likely

440 under sampled (aliased) by both the *in situ* measurements and the satellite observations used to re-analyse the fCO_2 data. In this case, reanalysis using an estimated or modelled skin temperature (based on the *in situ* SST at depth) may be more appropriate (see the discussion in Sect 2.4).
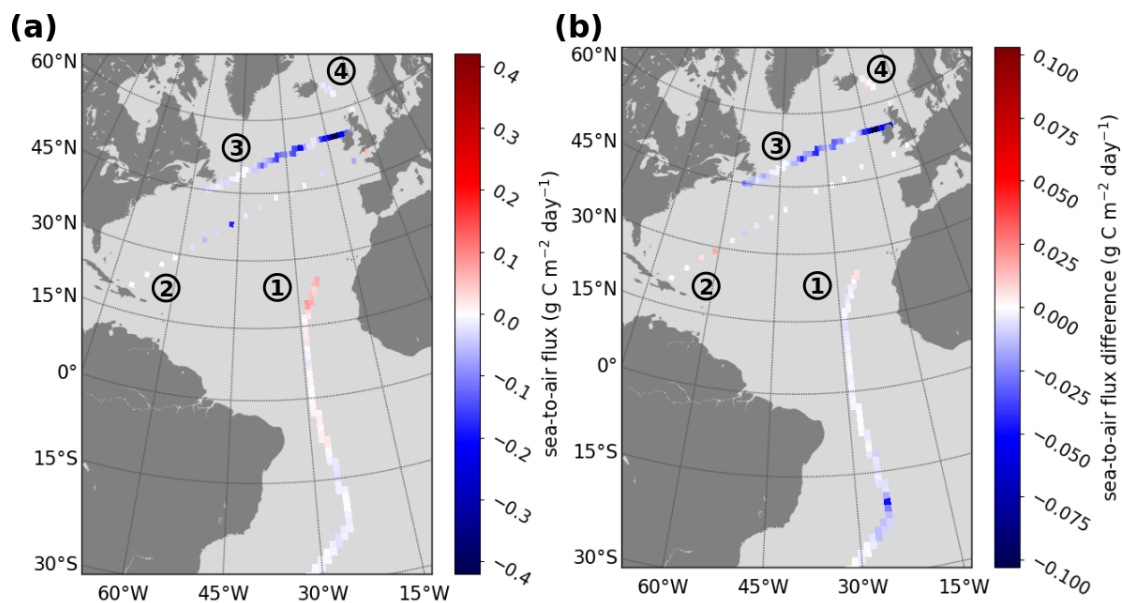
Figure 3: Example sea-to-air CO$_2$ fluxes calculated using *in situ* data and the gas transfer velocity detailed in Ho et al., (2006) (a) fluxes calculated for four sampling cruises in the North Atlantic during October and November 2013 (Kitidis and Brown, 2017; Schuster, 2016; Steinhoff *et al.*, 2016; Wanninkhof *et al.*, 2016) labelled 1-4, respectively. (b) The difference in the calculated flux resulting from using the reanalysed fCO$_2$ compared to the original *in situ* fCO$_2$ data (reanalysed minus original).

445   The *append2insitu.py* tool was then used to append FluxEngine output to the original input data file for the Kitidis and Brown (2017) dataset. The output from this tool enables the user to visualise FluxEngine output (including any additional input data such as the CCMP wind speed data) as a time series alongside all other *in situ* data. Figure 4 shows the time series of SST, fCO$_2$, and xCO$_2$ (from the downloaded cruise data). Plotted alongside these are the corresponding CCMP wind speed and the

450   calculated concentrations and fluxes using the original and reanalysed fCO$_2$ data.
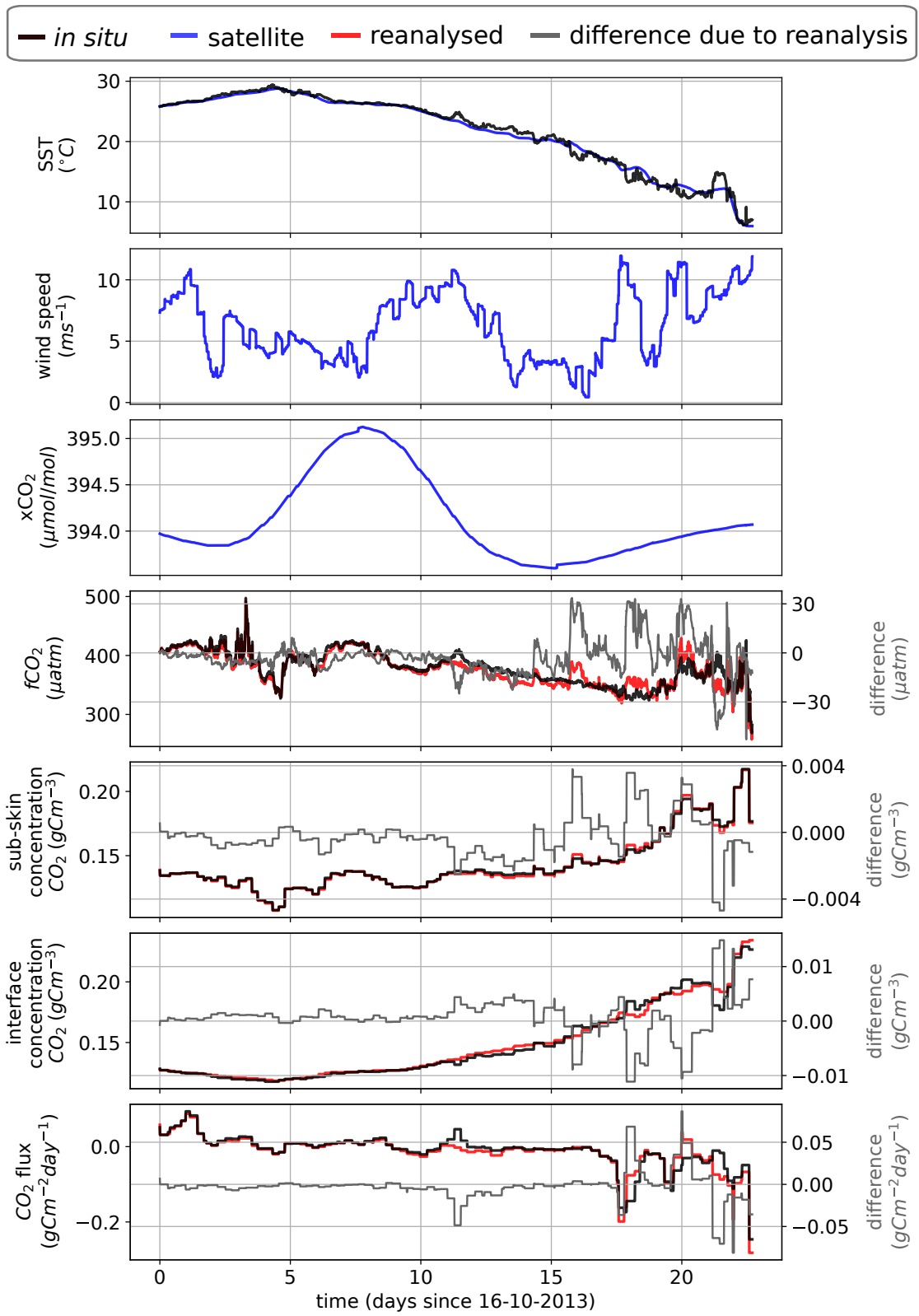
Figure 4: Time series of the (Kitidis and Brown, 2017) *in situ* **campaign data with the sea-to-air CO$_2$ flux as calculated by FluxEngine using the Ho** *et al.***, (2006) gas transfer velocity parameterisation. The results from the reanalysed fCO$_2$ values are shown in red to distinguish them from the original data. The differences in fCO$_2$, sub-skin and interface CO$_2$ concentration and sea-to-air CO$_2$ flux, resulting from the reanalysis, are shown in grey (reanalysed minus original).**

3.2 Case study 2: Calculating CO$_2$ fluxes from Östergarnsholm fixed station data

In this section the new capabilities for calculating gas fluxes from fixed stations is demonstrated using data from the long term monitoring station at Östergarnsholm. The Östergarnsholm station is situated in the Baltic Sea (57.42N, 18.99E) and is part of the Integrated Carbon Observation System (ICOS) infrastructure. The station was originally established in 1995 with the aim of collecting data on the marine atmospheric boundary layer to support research on the exchange of heat, momentum and CO_2 between the atmosphere and ocean. It is equipped with instruments to measure (amongst other parameters) profiles of wind speed, water temperature and aqueous fCO_2.

The new FluxEngine support for calculating gas fluxes from fixed stations uses the temporal dimension of the input files, creating output files of the same dimension that can be easily visualised as a time series. Data for the Östergarnsholm monitoring station covering a period from 28th January 2015 to the 9th September 2015 were downloaded from the data repository (Rutgersson, 2017). These data contain *in situ* measurements for fCO_2, salinity and temperature, model reanalysis air pressure at sea level from the National Center for Environmental Prediction and National Center for Atmospheric Research (NCEP/NCAR) dataset (Kalnay *et al*., 1996), xCO_2 from the NOAA ESRL GLOBALVIEW dataset (GLOBALVIEW-CO2, 2013) and World Ocean Atlas salinity data (Boyer *et al.*, 2013). CCMP wind speed data were extracted and added to the tab delimited *in situ* dataset using the same method as used in case study 1 (Sect. 3.1). For gridded input data values were extracted from the single grid point containing the Östergarnsholm station location was selected from a global 1° × 1° projected grid.

The *text2ncdf.py* tool was configured to convert the text formatted data file into a single netCDF file using a temporal resolution of one day. This produced a netCDF file with a temporal dimension size of 246 (days), containing the daily mean value for each of the 246 days covered by the dataset. For this case study FluxEngine was configured to use this file as input.

The flux calculation used the rapid model (Woolf *et al*., 2016) with the Nightingale *et al.* (2000) wind based gas transfer velocity parameterisation and was performed using the original *in situ* fCO_2 and SST data. The temporal resolution was set to provide daily calculations for each of the 246 days allowing seasonal variations to be observed. FluxEngine supports arbitrary temporal resolutions to within minute precision and the choice predominantly depends on the resolution of the available data and the particular research questions to be addressed. FluxEngine was configured to write output into a single netCDF file as a time series. The *in situ* fCO_2 and SST measurements were assumed to represent the conditions at the bottom of the mass boundary layer and the concentrations at the top of the mass boundary layer were estimated by configuring the FluxEngine to estimate the skin temperature using the *in situ* SST - 0.17 (which is based on the work of Donlon *et al.,* 2002).

Figure 5 shows the time series of SST, wind speed, xCO_2, fCO_2, concentration of CO_2 and calculated sea-to-air CO_2 flux. There is a moderate negative flux (ocean sink of CO_2) throughout most of the sampled period, which switched to a positive flux (outgassing to the atmosphere) during winter months. At approximately day 130 there is a local upwelling event which results in an incursion of CO_2 rich cold water. This results in an increase in fCO_2 of approximately 250 µatm, however coincident low wind speed means that there was little change in the flux during this event.
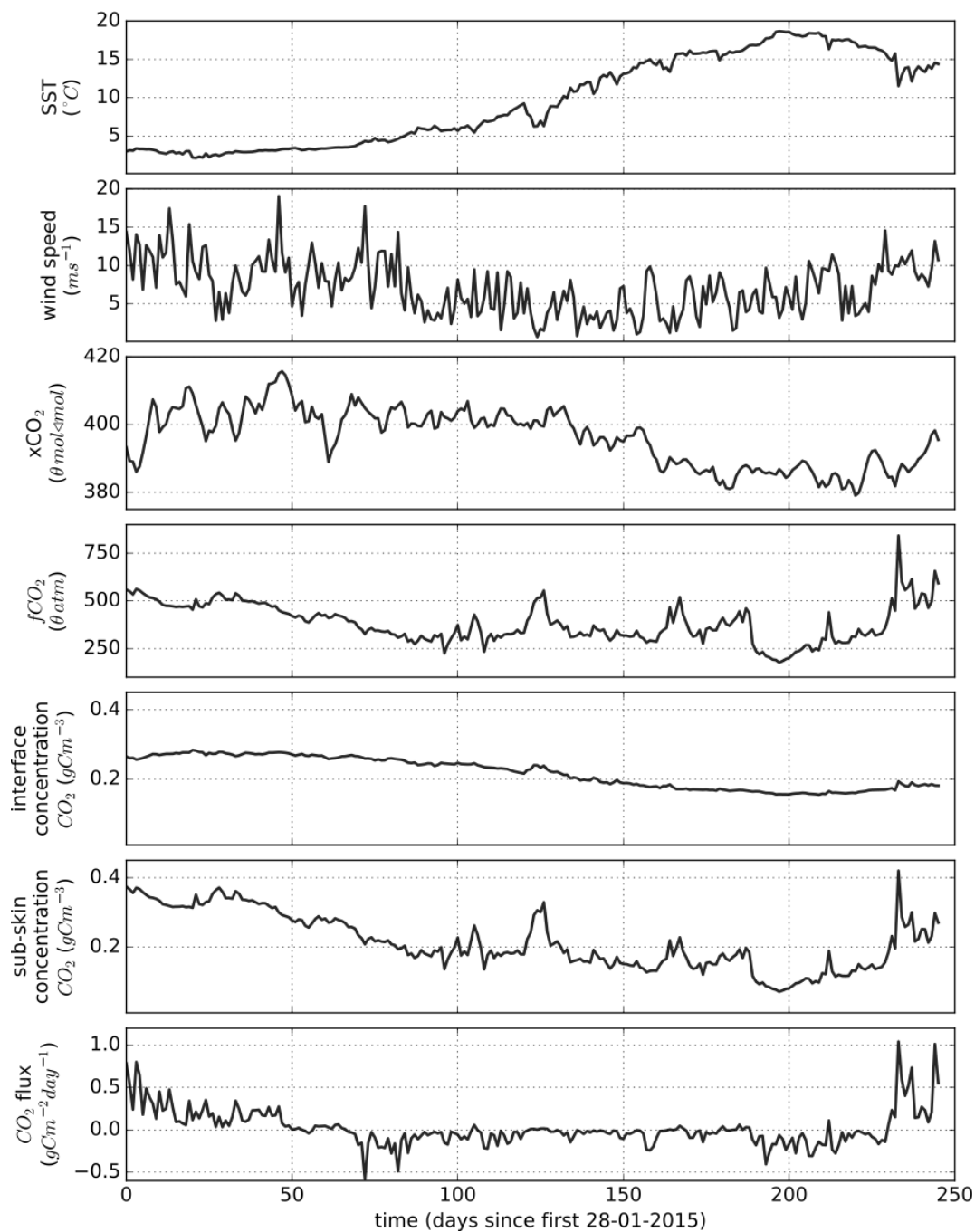
Figure 5: FluxEngine output file using data from Östergarnsholm station over the 246 day period. Example components of the sea-to-air flux calculation are shown alongside the calculated CO₂ flux.

3.3 Case study 3: Surfactant suppression of N_2O gas fluxes using the MEMENTO database

Nitrous oxide (N_2O) and methane (CH_4) are both climatically important gases. In the troposphere, they
act as greenhouse gases (IPCC, 2013), whereas stratospheric N_2O is the major source for nitric oxide
radicals which are involved in one of the main ozone reaction cycles (Ravishankara *et al.*, 2009).
Source estimates indicate that the world's oceans play a major role in the global budget of atmospheric
N_2O and a minor role in the case of CH_4 (IPCC, 2013). Oligotrophic ocean areas are near equilibrium
with the atmosphere and, consequently, make only a relatively small contribution to overall oceanic
emissions, whereas biologically productive regions (e.g., estuaries, shelf and coastal upwelling areas)
appear to be responsible for the major fraction of the N_2O and CH_4 emissions (Bakker *et al.*, 2014).

500

505

Surfactants are surface-active compounds that can suppress turbulence at the sea surface thus altering air-sea gas exchange (McKenna and Bock, 2006; Pereira *et al.*, 2016; Salter *et al.*, 2011). There is growing evidence from field and laboratory studies that naturally occurring surfactants can significantly reduce the flux of N_2O across the water/atmosphere interface (Kock *et al.*, 2012; Mesarchaki *et al.*, 2015).

Previous work, which studied CO_2 fluxes, found that surfactants potentially reduce the annual net integrated CO_2 flux by up to 9% in the Atlantic Ocean (Pereira *et al.*, 2018). Here, we use FluxEngine to apply the methodology of Pereira *et al.,* (2018) to *in situ* data from the MEMENTO (MarinE MethanE and NiTrous Oxide) database (Kock and Bange, 2015) in order to estimate the equivalent suppression effect on the exchange of N_2O between ocean and atmosphere.

While FluxEngine is able to calculate sea-to-air fluxes of both N_2O and CH_4, we confined our analysis to N_2O because of the sparsity of CH_4 data. *In situ* and 1° x 1° gridded monthly mean atmospheric and ocean partial pressure of N_2O, sea surface temperature and salinity were obtained from the MEMENTO database for the Atlantic Meridional Transect (AMT) cruise (AMT-24, JR303), which took place between September and November 2014 (Brown and Rees, 2018). These data were supplemented with Earth observation wind speed, U_{10}, from the CCMP dataset and modelled air pressure from the European Centre for Medium-Range Weather Forecasts (ECMWF). All input data were gridded to monthly means with a 1° x 1° resolution.

A custom gas transfer velocity parameterisation was implemented following the template provided in the toolbox to calculate the gas transfer suppression due to biological surfactants in surface waters. This parameterisation uses the gas transfer velocity of (Nightingale *et al.*, 2000) combined with an estimate of the degree of surfactant suppression from (Pereira *et al.*, 2018). The method described by Pereira *et al* used sea surface temperature to estimate surfactant suppression meaning that no additional input data fields were needed. FluxEngine was configured to use the rapid flux model (Woolf *et al.*, 2016) and run once with the standard Nightingale *et al.*, (2000) gas transfer parameterisation (no suppression case) and then again using the Pereira *et al.*, (2018) parameterisation (suppression case). This new gas transfer parameterisation is now freely available within the FluxEngine (and can be selected by specifying *k_Nightingale2000_with_surfactant_suppression* for the *k_parameterisation* option).

After calculating the air-to-sea N_2O fluxes we removed negative (atmosphere to ocean) fluxes. The fluxes for each grid cell (within which at least one *in situ* measurement exists) are shown in Fig. 6a, while the difference in sea-to-air flux due to surfactant suppression is shown in Fig. 6b. The largest fluxes occur in the tropics and sub-tropical part of the AMT cruise track (Fig. 6a). Suppression of the gas transfer reduces the magnitude of the air-sea flux and the largest absolute suppression is also seen in the tropics and sub-tropical regions (Fig. 6a and Fig. 6b).

The *append2insitu.py* utility was used to combine FluxEngine output with the original *in situ* data. The time series are shown in Fig. 6c for SST, wind speed, atmospheric and aqueous N_2O, and sea-to-air N_2O flux. The net fluxes along the transect are generally small and in both directions. The overall mean (and standard deviation) flux was 5.7×10^{-2} ($\pm 5.7 \times 10^{-2}$) g N_2O m^{-2} day^{-1} (no suppression) and 5.0×10^{-2}

$(\pm 4.8 \times 10^{-2})$ g N_2O m^{-2} day^{-1} (suppression), indicating in both cases a small net flux into the ocean. There was a mean flux suppression due to surfactants of 13% for the entire dataset.
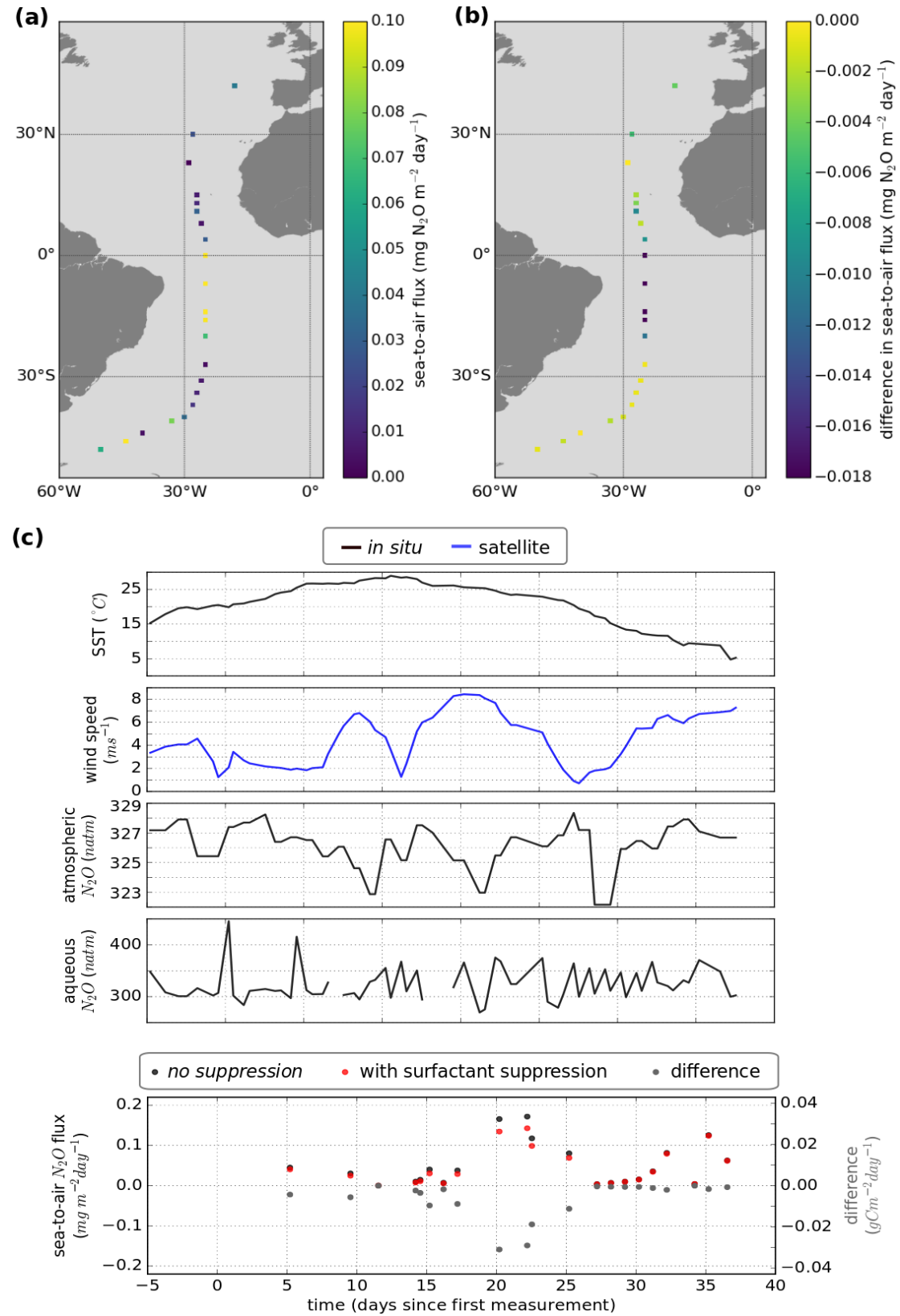
Figure 6: (a) Sea-to-air N_2O flux taking into account surfactant suppression. (b) Change in N_2O flux resulting from surfactant suppression. (c) Time series of SST, wind speed, atmospheric N_2O, aqueous N_2O and sea-to-air flux.

3.4 Case study 4: Gas transfer velocity parameterisation using turbulent kinetic energy
555   **dissipation rate**

The gas transfer velocity, k in equation 1 and 2, is determined by the turbulent mixing near the ocean surface (Jähne *et al.*, 1987). While it is common to estimate gas transfer using a polynomial relationship with wind speed, turbulence in the upper ocean is influenced by additional physical processes that are independent, or not solely dependent, on the wind. These include wave breaking,
560   shear stress due to geostrophic currents, wind-wave-current interactions, bottom-generated turbulence, tidal forces and precipitation (Villas Boas *et al.*, 2019; Zappa *et al.*, 2007; Zhao *et al.*, 2018).

In this case study we apply a turbulent kinetic energy dissipation rate (ε) based gas transfer velocity parameterisation, as developed by Zappa *et al.* (2007), to quantify the impact of wind- and wave-driven
565   turbulence on sea-to-air CO_2. Zappa *et al.* used direct measurements of k and ε in aquatic and shallow marine regions to derive the following relationship

$$k = 0.419 Sc^{-0.5}(\varepsilon v)^{0.25} \tag{3}$$

570   where k is the gas transfer velocity (m s^{-1}), Sc is the Schmidt number, ε is the turbulent kinetic energy dissipation rate (W kg^{-1}) and v is the kinematic viscosity of water (m^2 s^{-1}). We calculate the monthly mean ε using the monthly mean wave (swell, secondary swell and wind waves) to ocean turbulent kinetic energy flux (FOC) provided by the WAVEWATCH III model re-analysis (WAVEWATCH III development group, 2016). The mean dissipation rate of turbulent kinetic energy, ε_{mean}, is calculated
575   using ε_{mean} = FOC / (ρz_{max}), where ρ is the density of sea water (taken to be 1026 kg m^{-3}) and z_{max} is the maximum depth over which dissipation is assumed to occur (taken as 10 m from Fig. 8 of Craig and Banner, 1994). This provides the mean total dissipation rate through the volume of water. Equation 3 is valid for ε measurements near the surface (of the order of 0.1 to 0.2 m) and ε is known to decrease exponentially with depth. To estimate ε at a depth of 0.2 m we first fit an exponential function to the
580   curve of ε from Fig. 8 of Craig and Banner (1994) which gave:

$$\varepsilon = \beta \exp(0.20z + 0.78) \tag{4}$$

where z is depth and $\beta = 1.86 \times 10^{-3}$. Normalising this function to have a mean ε equal to ε_{mean} allows ε at
585   any depth to be determined. This was done by fitting β to minimise the difference between ε_{mean} calculated from FOC and ε_{mean} calculated from equation 4 to produce separate depth relationships with ε for each individual grid cell. Finally, the dissipation rate at 0.2 m was calculated by substituting z=0.2 into the final depth relationship. The process of fitting of the depth relationship and calculating ε at depth z=0.2 was implemented using a custom pre-processing function that is included as an example in
590   the FluxEngine download. This demonstrates how pre-processing functions can be used to perform complex data processing.

FluxEngine was then used to calculate monthly sea-to-air CO_2 fluxes, globally, for 2010. All inputs to FluxEngine were provided as monthly averages with a 1° x 1° resolution. The additional input data
595   were wind speed data from WAVEWATCH III re-analysis forcing field (WAVEWATCH III development group, 2016), sea surface temperature from Reynolds Optimally Interpolated Sea Surface Temperature dataset (OISST, Reynolds et al., 2007), salinity data from the NOAA World Ocean Atlas

(Zweng *et al.*, 2018), xCO_2 from the GLOBALVIEW CO_2 dataset (GLOBALVIEW-CO2, 2013), and fCO$_2$ data from the SOCAT derived sea-to-air CO_2 flux reference dataset for 2010 (Woolf *et al.*, 2019).

600   Since the Zappa *et al.*, (2007) relationship was parameterised in low to moderate wind speeds and in shallow marine environments, a mask was set in the configuration file to constrain the calculation to grid cells with wind speeds less than 10 m s^{-1} and shelf sea water depths between than 20 and 200 m, and then the analysis repeated with depths between 20 and 500 m. These depth ranges were chosen to be consistent with previous studies (e.g. Laruelle *et al.*, 2018; Shutler *et al.*, 2016), and the General

605   Bathymetric Chart of the Oceans (GEBCO) Digital Atlas bathymetry was used for this masking (GEBCO, 2003).

The *ofluxghg_flux_budgets.py* tool was used to compute the annual integrated net sea-to-air flux in all shelf sea regions. Collectively, the global shelf seas result in a net integrated flux into the ocean (sink)

610   of 0.57 to 0.78 Pg C for 2010, where the range is due to the two shelf definitions. These results are within the bounds of those determined by previous studies (0.2 – 1 PgC yr^{-1} from Laruelle *et al.*, 2018; Laruelle *et al.*, 2016). However we note that all previous studies have used wind speed for calculating gas exchange. Repeating the analysis with a wind speed based gas transfer velocity (Wanninkhof et al., 2014) instead of equation 4 gives an ~8% smaller net integrated flux of 0.53 to 0.72 Pg C. This result

615   could suggest that published values of the global shelf sea CO_2 sink (calculated using wind speed gas transfer) are underestimated, as they do not fully account for wind-wave-current interactions and whitecapping. Figure 7 shows the resulting mean annual sea-to-air CO_2 flux in 2010 for global shelf seas. The FluxEngine has the capability to use non-wind driven gas transfer parameterisations allowing more physically based approaches to be evaluated such as the use of ε. The first synoptic-scale

620   observation-based estimates of ε could soon be possible from space using Doppler techniques (e.g. Ardhuin *et al.,* 2019).
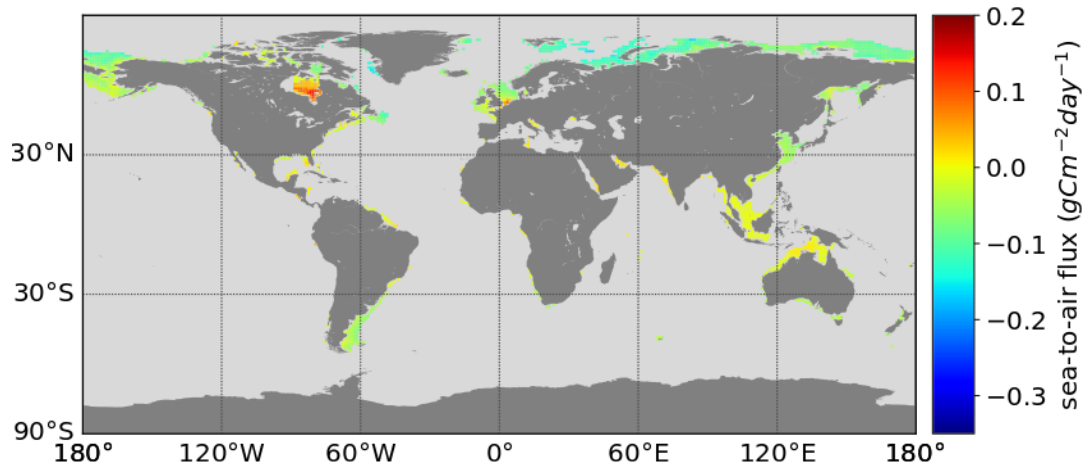
Figure 7: Mean annual sea-to-air CO$_2$ flux of shelf seas in 2010 using the Zappa et a al., (2007) gas transfer relationship for all regions and months with wind speeds 0 to 10 m s^{-1}. Shelf regions are defined as having depth between 20 m and 200 m.

625   **4. Future developments**
The FluxEngine toolbox will continue to be developed in response to new advances in research and further user-uptake will be encouraged through the provision of iPython Jupyter notebooks. There are currently four interactive Jupyter notebooks (tutorials) available within the FluxEngine v3.0 download

and these correspond to the first three case studies presented in this paper as well as an additional introductory tutorial. These interactive notebooks allow users to investigate the toolbox without the need to install any additional software. Users are able to modify and re-run the notebook and immediately see the impact of any changes. This approach has been previously used by the authors for supporting collaborative research and summer school teaching. Additional Jupyter notebooks could be written to provide worked examples of: i) driving FluxEngine with a custom Python script to perform a sensitivity or ensemble analysis, ii) using the FluxEngine to study a freshwater environment or iii) using the verification tools module to verify custom changes and extensions to the toolbox. All notebooks will be maintained so that they remain available and relevant to future versions of the FluxEngine.

5. Conclusions

The FluxEngine is an open-source and freely available software toolbox that provides standardised and verified calculations of gas exchange and net integrated fluxes between the ocean and atmosphere, and the toolbox is now being used by *in situ*, Earth observation and modelling scientific communities. The development of the toolbox was driven by the desire to reduce duplication of effort, to facilitate collaboration between different research communities, and thus to accelerate advancements in air-sea gas flux research and monitoring.

Building on Shutler *et al.,* (2016), which demonstrated the toolbox and verified the accuracy of the calculations, this paper demonstrates new capabilities that considerably broadens the scope of research questions that can be addressed using FluxEngine. Version 3.0 can now be easily installed and executed on a desktop or laptop computer and does not require specialist hardware or software libraries. It can be used as a Python library or as a set of stand-alone command line utilities. The toolbox now includes an extensive suite of tools for calculating gas fluxes directly from *in situ* data. Collectively, these improvements have streamlined the process for extending the toolbox and will allow users to easily take advantage of newly developed gas transfer velocity parameterisations and/or new sources of input data. These new tools and the toolbox are fully compatible with the internationally established data structures being used by the SOCAT and the MEMENTO communities.

The inclusion of the handling of CH_4 and N_2O sea-air gas fluxes is intended to directly support those communities studying these gases. Significant international research focus and effort is now being directed to collating data on these gases towards monitoring and understanding their spatial distribution and variability.

The FluxEngine toolbox will continue to be updated as new approaches become available. Further development will be guided by the needs of the international research and monitoring communities, and so we welcome feedback from users on all aspects of the toolbox.

Code availability

The FluxEngine software is open source and available on a creative commons license via http://github.com/oceanflux-ghg/FluxEngine. FluxEngine is in constant development and historic versions are available via GitHub. To access the specific version used to conduct the case studies in

section 3, please access the v3.0 release via: https://github.com/oceanflux-ghg/FluxEngine/releases/tag/v3.0

675

6. Appendix A: Utility names and descriptions

Several additional utilities are provided as Python scripts to support the installation, verification, execution and processing of output and these are listed in table 2.

Utility	Description
append2insitu.py	Appends netCDF data (e.g. FluxEngine output) to text formatted data files as new columns. Matching rows by longitude, latitude and time.
install_dependencies_macos.py, *install_dependencies_ubuntu.py*	Installation scripts. Installation instructions are provided for Windows users in *FluxEngineV3_instructions.pdf*
ncdf2text.py	Converts netCDF output files to text formatted files.
ofluxghg_flux_budgets.py	Calculates total monthly and annual gas flux from FluxEngine output. Supports global and regional analysis.
ofluxghg_run.py	Commandline tool used to run FluxEngine
reanalyse_socat_driver.py	Uses satellite sea surface temperature to reanalyse CO_2 fugacity and partial pressure data to a consistent temperature and depth (see Goddijn-Murphy *et al.,* 2015)
run_full_verification.py	Runs an extended verification procedure. Required additional data from (Holding *et al.*, 2018)
text2ncdf.py	Converts text formatted data files into FluxEngine compatible netCDF format.
validation_tools.py, compare_net_budgets.py	Contains Python functions to aid verification of FluxEngine output to a reference dataset.
verify_socatv4_sst_salinity_gradients_N00.py, *verify_takahashi09.py*	Verifies that FluxEngine has been installed correctly by comparing output with a reference data from SOCAT-derived or Takahashi climatologies, respectively.

680 **Table 2:** Description of the bundled tools and scripts that are included in FluxEngine. Each tool can be used as a stand-alone command line tool or used as a Python package.

685 ## 7. Appendix B: Datasets used

Table 3 provides details of each of the data sets that were used in the case studies.

Name	Parameter(s)	Reference/source
CCMP v2 (Cross-Calibrated Multi-Platform)	U_{10} (wind speed at 10m)	Atlas *et al.*, 2011 http://www.remss.com/measurements/ccmp/
OISST (Optimally-Interpolated Seas Surface Temperature)	Sea surface temperature (SST)	Reynolds *et al.*, 2007 https://www.ncdc.noaa.gov/oisst
GLOBALVIEW CO_2	xCO_2 (molar fraction of CO_2 in dry air)	GLOBALVIEW-CO2, 2013 https://www.esrl.noaa.gov/gmd/ccgg/globalview/co2/co2_intro.html
National Centers for Environmental Prediction, National Center for	Air pressure	Kalnay *et al.*, 1996 https://www.esrl.noaa.gov/psd/data/gridded/data.ncep.reanalysis.pressure.html

Atmospheric Research (NCEP/NCAR)		
Underway data from the James Clark cruise (74JC20131009)	SST, salinity, air pressure, fCO_2	Kitidis and Brown, 2017 https://doi.pangaea.de/10.1594/PANGAEA.878492
Underway data from the Belguela Stream cruise (642B20131005)	SST, salinity, air pressure, fCO_2	Schuster, 2016 https://doi.org/10.1594/PANGAEA.852980
Underway data from the Atlantic Companion cruise (77CN20131004)	SST, salinity, air pressure, fCO_2	Steinhoff *et al.*, 2016 https://doi.org/10.1594/PANGAEA.852786
Underway data from the REYJAFOSS cruise (64RJ20131017)	SST, salinity, air pressure, fCO_2, xCO_2	Wanninkhof *et al.*, 2016 https://doi.org/10.1594/PANGAEA.866092
Östergarnsholm station (77FS20150128)	Air pressure, salinity, SST, xCO_2 (air), fCO_2 (water)	Rutgersson, 2017 https://doi.pangaea.de/10.1594/PANGAEA.878531
MarinE MethanE and NiTrous Oxide database (MEMENTO)	SST, pN_2O_{air}, pN_2O_{water},	Kock and Bange, 2015 https://memento.geomar.de/
National Oceanic and Atmospheric Administration, US (NOAA) WAVEWATCH III	U_{10} (wind speed at 10m), FOC (wave to turbulent kinetic energy)	WAVEWATCH III development group, 2016

Table 3: The Earth observation *in situ*, model and climatology data used in this research.

8. Appendix C Summary of main toolbox features

Table 4 lists the main features of the FluxEngine toolbox with summaries of their impact for the accurate calculation of atmosphere-ocean gas fluxes.

Feature or option	Description	Example impact or use
Ability to choose the structure of the bulk gas flux calculation or formulation	The user can choose their bulk formulation, but a formulation based on concentration differences (i.e. containing two solubilities) is advised. This advised formulation enables near-surface temperature and salinity gradients to be included. For reasoning and examples of this advice please see Woolf *et al.* (2016), Woolf *et al.,* (2019). and Section 1b of Shutler *et al.* (2016).	Woolf et al., (2019) shows that ignoring vertical temperature and salinity gradients for 2010 results in a 0.35 PgC (12%) bias or underestimate in the oceanic sink of CO_2.
User selectable gas transfer velocity parameterisations	The toolbox includes 14 published wind speed parameterisations and one mean square slope parameterisation , along with a generic user-configurable wind speed parameterisation (see section 7 of the FluxEngine manual). Custom user parameterisations can be added using	Wrobel and Piskozub (2016) showed that the (model) uncertainty due to the choice of quadratic gas transfer parameterisation led to 9% difference in the gas transfer velocity for the North Atlantic and sub polar waters. This uncertainty increased to 65% when all parameterisations were

	a Python template (section 9.2 of the FluxEngine manual).	considered.
Reanalyse fCO$_2$ data to a reference temperature and depth	The user can reanalyse paired *in situ* fCO$_2$ and SST measurements to a consistent depth using a reference temperature dataset as described by Goddijn-Murphy *et al.* (2015).	This removes unknown biases due to paired data originating from multiple depths. The depth of in situ data can vary during a single research cruise (e.g. due to sea state or ballasting) and measurements from varying depths becomes a more significant problem when using large collated datasets collected using different measurement systems.
User selectable gas input data types	The user can input atmospheric and marine gas data as partial pressures, fugacities or concentrations.	Allows a wider range of poorly soluble gases to be analysed.
Flexibility to calculate air-sea gas fluxes of multiple poorly soluble gases	The toolbox supports user definable sea-to-air gas flux calculations for CO$_2$, CH$_4$ and N$_2$O.	This paper estimates that surfactants can suppress N$_2$O gas fluxes by up to 13% in the North Atlantic.
Accounting for the impact of rain on air-sea gas fluxes	Users can investigate methods that include the different influences that rain can have on air-sea gas fluxes.	Ashton et al., (2016) estimated that rain driven gas transfer and wet deposition of carbon increases the annual oceanic integrated net sink of CO$_2$ by up to 6%.
Flexible input data specification and support for *in situ* data	Tools are provided to support user-specified grid size, temporal resolution, naming conventions and directory structure, automatic unit conversion and conversion between text (ASCII) and netCDF formatted data files.	Allows a wide range of data to be easily used and analysed by the user and the FluxEngine outputs can be easily incorporated into the users original *in situ* dataset.
Calculate integrated net gas fluxes	A tool for calculating global or regional integrated net gas fluxes (e.g. CO$_2$ sink) from netCDF air-sea gas flux data is provided. This enables user defined land, ice and region of interest masks to be used and there are multiple options for handling the impact of sea ice.	Shutler *et al.* (2016) showed that the calculated net CO$_2$ fluxes can vary by 14% for the European shelf sea simply due to differing shelf sea masks, highlighting the need for traceable methods and masks for net flux calculations.
Input data uncertainty analysis	Users can add random noise (with user defined variance and bias) to any input dataset. This enables the users to investigate the impact of input data uncertainties on their air-sea gas flux calculation (e.g. through using an ensemble approach)	Ashton et al. (2016) identified that known uncertainties due to random fluctuations in the input data resulted in a ±1% variation in the monthly net integrated CO$_2$ sink. Land et al. (2013) identified that the dominant source of uncertainty in Arctic air-sea gas flux calculations was due to bias in wind speed data (and its impact on the wind speed based gas transfer velocity).

Table 4: An overview of the key features provided by the FluxEngine software toolkit and their relevance or use for atmosphere-ocean gas exchange.

695

Author contributions

Design and analysis performed by T. Holding, I. Ashton and J. Shutler. Software engineering performed by T. Holding and I. Ashton. Pre-processing of nitrous oxide data performed by A. Kock. All authors contributed to the preparation of the manuscript.

700

Acknowledgements

This work was partially funded by the European Space Agency (ESA) Support to Science Element (STSE) through the OceanFlux Greenhouse Gases project (contract 4000104762/11/I-AM), the OceanFlux Greenhouse Gases Evolution project (contract 4000112091/14/I-LG), and by the European Space Agency (ESA) through the Sea surface Kinematics Multiscale monitoring (SKIM) Mission Science study (contract 4000124734/18/NL/CT/gp) and the ESA SKIM Scientific Performance Evaluation study (contract 4000124521/18/NL/CT/gp), as well as through the NERC RAGNARoCC project, (grant ref. NE/K002473/1). Further development of FluxEngine was funded by the European Union's Seventh Programme for Research and Technology Development (grant no. 03FO773A (BONUS INTEGRAL) and grant no. 730944 (RINGO)).

The Surface Ocean CO_2 Atlas (SOCAT) is an international effort, endorsed by the International Ocean Carbon Coordination Project (IOCCP), the Surface Ocean Lower Atmosphere Study (SOLAS) and the Integrated Marine Biosphere Research (IMBeR) program, to deliver a uniformly quality-controlled surface ocean CO_2 database. The many researchers and funding agencies responsible for the collection of data and quality control are thanked for their contributions to SOCAT.

CCMP Version-2.0 vector wind analyses are produced by Remote Sensing Systems (http://www.remss.com). NCEP Reanalysis data provided by the NOAA/OAR/ESRL PSD, Boulder, Colorado, USA, from their web site at https://www.esrl.noaa.gov/psd/.

MEMENTO (https://memento.geomar.de/) is currently supported by the Kiel Data Management Team at GEOMAR and the BONUS INTEGRAL Project.

This study is a contribution to the international IMBeR project and was supported by the UK Natural Environment Research Council National Capability (CLASS Theme 1.2) funding to Plymouth Marine Laboratory. This is contribution number 330 of the AMT programme.

BONUS INTEGRAL receives funding from BONUS (Art 185), funded jointly by the EU, the German Federal Ministry of Education and Research, the Swedish Research Council Formas, the Academy of Finland, the Polish National Centre for Research and Development, and the Estonian Research Council.

Competing interests

The authors declare that they have no conflict of interest.

735

References

Ardhuin, F., Aksenov, Y., Benetazzo, A., Bertino, L., Brandt, P., Caubet, E., Chapron, B., Collard, F., Cravatte, S., Delouis, J.-M., Dias, F., Dibarboure, G., Gaultier, L., Johannessen, J., Korosov, A., Manucharyan, G., Menemenlis, D., Menendez, M., Monnier, G., Mouche, A., Nouguier, F., Nurser, G., Rampal, P., Reniers, A., Rodriguez, E., Stopa, J., Tison, C., Ubelmann, C., van Sebille, E. and Xie, J.: Measuring currents, ice drift, and waves from space: the Sea surface KInematics Multiscale monitoring (SKIM) concept, Ocean Sci., 14(3), 337–354, doi:10.5194/os-14-337-2018, 2018.

Ashton, I. G., Shutler, J. D., Land, P. E., Woolf, D. K. and Quartly, G. D.: A Sensitivity Analysis of the

Impact of Rain on Regional and Global Sea-Air Fluxes of CO2, edited by M. deCastro, PLoS One, 11(9), e0161105, doi:10.1371/journal.pone.0161105, 2016.

750 Atlas, R., Hoffman, R. N., Ardizzone, J., Leidner, S. M., Jusem, J. C., Smith, D. K. and Gombos, D.: A Cross-calibrated, Multiplatform Ocean Surface Wind Velocity Product for Meteorological and Oceanographic Applications, Bull. Am. Meteorol. Soc., 92(2), 157–174, doi:10.1175/2010BAMS2946.1, 2011.

755 Bakker, D. C. E., Bange, H. W., Gruber, N., Johannessen, T., Upstill-Goddard, R. C., Borges, A. V., Delille, B., Löscher, C. R., Naqvi, S. W. A., Omar, A. M. and Santana-Casiano, J. M.: Air-Sea Interactions of Natural Long-Lived Greenhouse Gases (CO2, N2O, CH4) in a Changing Climate, pp. 113–169, Springer, Berlin, Heidelberg., 2014.

760 Bakker, D. C. E., Pfeil, B., Landa, C. S., Metzl, N. O., Brien, K. M., Olsen, A., Smith, K., Cosca, C., Harasawa, S., Jones, S. D., Nakaoka, S., Nojiri, Y., Schuster, U., Steinhoff, T., Sweeney, C., Takahashi, T., Tilbrook, B., Wada, C., Wanninkhof, R., Alin, S. R., Balestrini, C. F., Barbero, L., Bates, N. R., Bianchi, A. A., Bonou, F., Boutin, J., Bozec, Y., Burger, E. F., Cai, W.-J., Castle, R. D., Chen, L., Chierici, M., Currie, K., Evans, W., Featherstone, C., Feely, R. A., Fransson, A., Goyet, C., Greenwood, N., Gregor, L., Hankin, S., Hardman-Mountford, N. J., Harlay, J., Hauck, J., Hoppema,
765 M., Humphreys, M. P., Hunt, C. W., Huss, B., Ibánhez, J. S. P., Johannessen, T., Keeling, R., Kitidis, V., Körtzinger, A., Kozyr, A., Krasakopoulou, E., Kuwata, A., Landschützer, P., Lauvset, S. K., Lefèvre, N., Lo Monaco, C., Manke, A., Mathis, J. T., Merlivat, L., Millero, F. J., Monteiro, P. M. S., Munro, D. R., Murata, A., Newberger, T., Omar, A. M., Ono, T., Paterson, K., Pearce, D., Pierrot, D., Robbins, L. L., Saito, S., Salisbury, J., Schlitzer, R., Schneider, B., Schweitzer, R., Sieger, R., Skjelvan,
770 I., Sullivan, K. F., Sutherland, S. C., Sutton, A. J., Tadokoro, K., Telszewski, M., Tuma, M., van Heuven, S. M. A. C., Vandemark, D., Ward, B., Watson, A. J. and Xu, S.: A multi-decade record of high-quality fCO2 data in version 3 of the Surface Ocean CO2 Atlas (SOCAT), Earth Syst. Sci. Data, 8(2), 383–413, doi:10.5194/essd-8-383-2016, 2016.

775 Boyer, T.P., J. I. Antonov, O. K. Baranova, C. Coleman, H. E. Garcia, A. Grodsky, D. R. Johnson, R. A. Locarnini, A. V. Mishonov, T.D. O'Brien, C.R. Paver, J.R. Reagan, D. Seidov, I. V. Smolyar, and M. M. Z.: World Ocean Database 2013, NOAA Atlas NESDIF, 72, 209, doi:10.7289/V5NZ85MT, 2013.

780 Brown, I. and Rees, A.: Nitrous Oxide measurements from CTD collected depth profiles along a North-South transect in the Atlantic Ocean on cruise JR303/AMT24/JR20140922, Br. Oceanogr. Data Cent. - Nat. Environ. Res. Counc. UK, doi:10.5285/7cbed206-c122-2777-e053-6c86abc041f9, 2018.

785 Craig, P. D., Banner, M. L. and Craig, P. D.: Modeling Wave-Enhanced Turbulence in the Ocean Surface Layer, J. Phys. Oceanogr., 24(12), 2546–2559, doi:10.1175/1520-0485(1994)024<2546:MWETIT>2.0.CO;2, 1994.

790 Donlon, C., Robinson, I. S., Wimmer, W., Fisher, G., Reynolds, M., Edwards, R. and Nightingale, T. J.: An Infrared Sea Surface Temperature Autonomous Radiometer (ISAR) for Deployment aboard Volunteer Observing Ships (VOS), J. Atmos. Ocean. Technol., 25(1), 93–113, doi:10.1175/2007JTECHO505.1, 2008.

795 Fairall, C. W., Bradley, E. F., Rogers, D. P., Edson, J. B. and Young, G. S.: Bulk parameterization of air-sea fluxes for Tropical Ocean-Global Atmosphere Coupled-Ocean Atmosphere Response Experiment, J. Geophys. Res. Ocean., 101(C2), 3747–3764, doi:10.1029/95JC03205, 1996.

GEBCO: The GEBCO Digital Atlas published by the British Oceanographic Data Centre on behalf of IOC and IHO, 2003.

800 GLOBALVIEW-CO2: Cooperative Global Atmospheric Data Integration Project. 2013, updated annually. Multi-laboratory compilation of synchronized and gap-filled atmospheric carbon dioxide records for the period 1979-2012 (obspack_co2_1_GLOBALVIEW-CO2_2013_v1.0.4_2013-12-23), Compil. by NOAA Glob. Monit. Devision, doi:10.3334/OBSPACK/1002, 2013.

805 Goddijn-Murphy, L. M., Woolf, D. K., Land, P. E., Shutler, J. D. and Donlon, C.: The OceanFlux Greenhouse Gases methodology for deriving a sea surface climatology of CO2 fugacity in support of air–sea gas flux studies, Ocean Sci., 11(4), 519–541, doi:10.5194/os-11-519-2015, 2015.

810 Henson, S. A., Humphreys, M. P., Land, P. E., Shutler, J. D., Goddijn-Murphy, L. and Warren, M.: Controls on open-ocean North Atlantic ΔpCO2 at seasonal and interannual timescales are different, Geophys. Res. Lett., 45(17), 9067–9076, doi:10.1029/2018GL078797, 2018.

Ho, D. T., Law, C. S., Smith, M. J., Schlosser, P., Harvey, M. and Hill, P.: Measurements of air-sea gas exchange at high wind speeds in the Southern Ocean: Implications for global parameterizations, Geophys. Res. Lett., 33(16), L16611, doi:10.1029/2006GL026817, 2006.

Ho, D. T., Veron, F., Harrison, E., Bliven, L. F., Scott, N. and McGillis, W. R.: The combined effect of rain and wind on air–water gas exchange: A feasibility study, J. Mar. Syst., 66(1–4), 150–160, doi:10.1016/J.JMARSYS.2006.02.012, 2007.

Holding, Thomas; Ashton, Ian; Woolf, David K; Shutler, J. D.: FluxEngine v2.0 and v3.0 reference and verification data, PANGAEA, doi:10.1594/PANGAEA.890118, 2018.

IPCC: Climate Change 2013: The Physical Science Basis. Contribution of Working Group I to the Fifth Assessment Report of the Intergovernmental Panel on Climate Change, edited by V. B. and P. M. M. Stocker, T.F., D. Qin, G.-K. Plattner, M. Tignor, S.K. Allen, J. Boschung, A. Nauels, Y. Xia, Cambridge University Press, Cambridge, United Kingdom and New York, NY, USA, 1535 pp. [online] Available from: https://www.ipcc.ch/report/ar5/wg1/, 2013.

Jähne, B., Münnich, K. O., Bösinger, R., Dutzi, A., Huber, W. and Libner, P.: On the parameters influencing air-water gas exchange, J. Geophys. Res., 92(C2), 1937, doi:10.1029/JC092iC02p01937, 1987.

Kalnay, E., Kanamitsu, M., Kistler, R., Collins, W., Deaven, D., Gandin, L., Iredell, M., Saha, S., White, G., Woollen, J., Zhu, Y., Leetmaa, A., Reynolds, R., Chelliah, M., Ebisuzaki, W., Higgins, W., Janowiak, J., Mo, K. C., Ropelewski, C., Wang, J., Jenne, R., Joseph, D., Kalnay, E., Kanamitsu, M., Kistler, R., Collins, W., Deaven, D., Gandin, L., Iredell, M., Saha, S., White, G., Woollen, J., Zhu, Y., Chelliah, M., Ebisuzaki, W., Higgins, W., Janowiak, J., Mo, K. C., Ropelewski, C., Wang, J., Leetmaa, A., Reynolds, R., Jenne, R. and Joseph, D.: The NCEP/NCAR 40-Year Reanalysis Project, Bull. Am. Meteorol. Soc., 77(3), 437–471, doi:10.1175/1520-0477(1996)077<0437:TNYRP>2.0.CO;2, 1996.

Kitidis, Vassilis; Brown, I.: Underway physical oceanography and carbon dioxide measurements during James Clark Ross cruise 74JC20131009, PANGAEA, doi:10.1594/PANGAEA.878492, 2017.
Kock, A. and Bange, H.: Counting the Ocean's Greenhouse Gas Emissions, Earth Sp. Sci. News, 96, doi:10.1029/2015EO023665, 2015.

Kock, A., Schafstall, J., Dengler, M., Brandt, P. and Bange, H. W.: Sea-to-air and diapycnal nitrous oxide fluxes in the eastern tropical North Atlantic Ocean, Biogeosciences, 9(3), 957–964, doi:10.5194/bg-9-957-2012, 2012.

Laruelle, G. G., Cai, W.-J., Hu, X., Gruber, N., Mackenzie, F. T. and Regnier, P.: Continental shelves as a variable but increasing global sink for atmospheric carbon dioxide., Nat. Commun., 9(1), 454, doi:10.1038/s41467-017-02738-z, 2018.

M. M. Zweng, Reagan, J. R., Seidov, D., Boyer, T. P., Locarnini, R. A., Garcia, H. E., Mishonov, A. V., Baranova, O. K., Weathers, K., Paver, C. R. and Smolyar, I.: WORLD OCEAN ATLAS 2018 Volume 2: Salinity (pre-release). [online] Available from: http://www.nodc.noaa.gov/ (Accessed 26 March 2019), 2018.

McKenna, S. P. and Bock, E. J.: Physicochemical effects of the marine microlayer on air-sea gas transport, in Marine Surface Films, pp. 77–91, Springer-Verlag, Berlin/Heidelberg., 2006.

Mesarchaki, E., Kräuter, C., Krall, K. E., Bopp, M., Helleis, F., Williams, J. and Jähne, B.: Measuring air–sea gas-exchange velocities in a large-scale annular wind–wave tank, Ocean Sci., 11(1), 121–138, doi:10.5194/os-11-121-2015, 2015.

Nightingale, P. D., Malin, G., Law, C. S., Watson, A. J., Liss, P. S., Liddicoat, M. I., Boutin, J. and Upstill-Goddard, R. C.: In situ evaluation of air-sea gas exchange parameterizations using novel conservative and volatile tracers, Global Biogeochem. Cycles, 14(1), 373–387, doi:10.1029/1999GB900091, 2000.

Pereira, R., Schneider-Zapp, K. and Upstill-Goddard, R. C.: Surfactant control of gas transfer velocity along an offshore coastal transect: results from a laboratory gas exchange tank, Biogeosciences, 13(13), 3981–3989, doi:10.5194/bg-13-3981-2016, 2016.

Pereira, R., Ashton, I., Sabbaghzadeh, B., Shutler, J. D. and Upstill-Goddard, R. C.: Reduced air–sea CO2 exchange in the Atlantic Ocean due to biological surfactants, Nat. Geosci., 11(7), 492–496,

doi:10.1038/s41561-018-0136-2, 2018.

880   Ravishankara, A. R., Daniel, J. S. and Portmann, R. W.: Nitrous oxide (N2O): the dominant ozone-depleting substance emitted in the 21st century., Science, 326(5949), 123–5, doi:10.1126/science.1176985, 2009.

Reynolds, R. W., Smith, T. M., Liu, C., Chelton, D. B., Casey, K. S. and Schlax, M. G.: Daily High-
885   Resolution-Blended Analyses for Sea Surface Temperature, J. Clim., 20(22), 5473–5496, doi:10.1175/2007JCLI1824.1, 2007.

Rödenbeck, C., Bakker, D. C. E., Gruber, N., Iida, Y., Jacobson, A. R., Jones, S., Landschützer, P., Metzl, N., Nakaoka, S., Olsen, A., Park, G.-H., Peylin, P., Rodgers, K. B., Sasse, T. P., Schuster, U.,
890   Shutler, J. D., Valsala, V., Wanninkhof, R. and Zeng, J.: Data-based estimates of the ocean carbon sink variability - First results of the Surface Ocean pCO2 Mapping intercomparison (SOCOM), Biogeosciences, 12(23), 7251–7278, doi:10.5194/bg-12-7251-2015, 2015.

Rutgersson, A.: Time series of physical oceanography and carbon dioxide measurements at mooring
895   site OSTERGARNSHOLM - 77FS20150128, PANGAEA, doi:10.1594/PANGAEA.878531, 2017.

Salter, M. E., Upstill-Goddard, R. C., Nightingale, P. D., Archer, S. D., Blomquist, B., Ho, D. T., Huebert, B., Schlosser, P. and Yang, M.: Impact of an artificial surfactant release on air-sea gas fluxes during Deep Ocean Gas Exchange Experiment II, J. Geophys. Res., 116(C11), C11016,
900   doi:10.1029/2011JC007023, 2011.

Schuster, U.: Underway physical oceanography and carbon dioxide measurements during Benguela Stream cruise 642B20131005, PANGAEA, doi:10.1594/PANGAEA.852980, 2016.

905   Shutler, J. D., Land, P. E., Piolle, J. F., Woolf, D. K., Goddijn-Murphy, L., Paul, F., Girard-Ardhuin, F., Chapron, B. and Donlon, C. J.: FluxEngine: A flexible processing system for calculating atmosphere-ocean carbon dioxide gas fluxes and climatologies, J. Atmos. Ocean. Technol., 33(4), 741–756, doi:10.1175/JTECH-D-14-00204.1, 2016.

910   Steinhoff, Tobias; Becker, Meike; Körtzinger, A.: Underway physical oceanography and carbon dioxide measurements during Atlantic Companion cruise 77CN20131004, PANGAEA, doi:10.1594/PANGAEA.852786, 2016.

Takahashi, T., Sutherland, S. C., Wanninkhof, R., Sweeney, C., Feely, R. A., Chipman, D. W., Hales,
915   B., Friederich, G., Chavez, F., Sabine, C., Watson, A., Bakker, D. C. E., Schuster, U., Yoshikawa-Inoue, H., Ishii, M., Midorikawa, T., Nojiri, Y., Körtzinger, A., Steinhoff, T., Hoppema, M., Olafsson, J., Arnarson, T. S., Johannessen, T., Olsen, A., Bellerby, R., Wong, C. S., Delille, B., Bates, N. R. and de Baar, H. J. W.: Climatological mean and decadal change in surface ocean pCO2, and net sea–air CO2 flux over the global oceans, Deep Sea Res. Part II Top. Stud. Oceanogr., 56(8–10), 554–577,
920   doi:10.1016/J.DSR2.2008.12.009, 2009.

Tarran, G.: AMT 28 Cruise Report. [online] Available from: https://amt-uk.org/getattachment/Cruises/AMT28/AMT_28_CRUISE_REPORT_RS.pdf, 2018.

925   Wanninkhof, Rik; Pierrot, D.: Underway physical oceanography and carbon dioxide measurements during REYKJAFOSS cruise 64RJ20131017, PANGAEA, doi:10.1594/PANGAEA.866092, 2016. Wanninkhof, R.: Relationship between wind speed and gas exchange over the ocean, J. Geophys. Res., 97(C5), 7373, doi:10.1029/92JC00188, 1992.

930   Wanninkhof, R.: Relationship between wind speed and gas exchange over the ocean revisited, Limnol. Oceanogr. Methods, 12(6), 351–362, doi:10.4319/lom.2014.12.351, 2014. WAVEWATCH III development group: User manual and system documentation of WAVEWATCH III version 5.16, Technical Note 329., 2016.

935   Woolf, D. K., Land, P. E., Shutler, J. D., Goddijn-Murphy, L. M. and Donlon, C. J.: On the calculation of air-sea fluxes of CO_2 in the presence of temperature and salinity gradients, J. Geophys. Res. Ocean., 121(2), 1229–1248, doi:10.1002/2015JC011427, 2016.

Woolf, D. K., Shutler, J. D., Goddijn-Murphy, L., Watson, A. J., Chapron, B., Nightingale, P. D.,
940   Donlon, C. J., Piskozub, J., Yelland, M. J., Ashton, I., Holding, T., Schuster, U., Girard-Ardhuin, F., Grouazel, A., Piolle, J. -F., Warren, M., Wrobel-Niedzwiecka, I., Land, P. E., Torres, R., Prytherch, J., Moat, B., Hanafin, J., Ardhuin, F. and Paul, F.: Key Uncertainties in the Recent Air-Sea Flux of CO2,

Global Biogeochem. Cycles, 0–3, doi:10.1029/2018gb006041, 2019.

945   Wrobel, I.: Monthly dynamics of carbon dioxide exchange across the sea surface of the Arctic Ocean in response to changes in gas transfer velocity and partial pressure of CO2 in 2010, Oceanologia, 59(4), 445–459, doi:10.1016/J.OCEANO.2017.05.001, 2017.

       Wrobel, I. and Piskozub, J.: Effect of gas-transfer velocity parameterization choice on air-sea CO2
950   fluxes in the North Atlantic Ocean and the European Arctic, Ocean Sci., 12(5), 1091–1091, 2016.

       Zappa, C. J., McGillis, W. R., Raymond, P. A., Edson, J. B., Hintsa, E. J., Zemmelink, H. J., Dacey, J. W. H. and Ho, D. T.: Environmental turbulent mixing controls on air-water gas exchange in marine and aquatic systems, Geophys. Res. Lett., 34(10), L10601, doi:10.1029/2006GL028790, 2007.
955

       Zhao, D., Jia, N. and Dong, Y.: Relationship between turbulent energy dissipation and gas transfer through the air–sea interface, Tellus B Chem. Phys. Meteorol., 70(1), 1–11, doi:10.1080/16000889.2018.1528133, 2018.